Nonlinear Dynamic Behavior of a Piezoelectric 1-3 Composite

Thomas J. Royston* and Brian H. Houston*

*University of Illinois at Chicago, Chicago, IL 60601 and *Naval Research Laboratory, Washington, D.C., 20375

Abstract: The nonlinear vibratory behavior of a smart material component, a 1-3 piezoceramic composite, is characterized. Dynamic experimental measurements of the 1-3's mechanical response to harmonic electrical excitation over a range of excitation frequencies and mechanical loading conditions quantify the level of harmonic distortion in the device.

INTRODUCTION

To meet needs for improved transduction and control there has been much research on the use of so-called smart materials and structures with integrated actuation and sensing which enable a greater ability to manipulate and measure vibro-acoustic energy. Though all dynamic systems are inherently nonlinear, the majority of analyses are typically based on the assumption of linearity. While vibration of conventional (nonsmart) systems is often reasonably described by linear system theory, particularly in the audio and ultrasonic frequency ranges, the dynamics of systems employing smart materials often are not, whether they be based on piezoelectric, electrostrictive, magnetostrictive, or electro-rheological technologies. Nonlinearities can affect the system performance through a loss of actuation authority, stability, and/or system functionality. Alternatively, an intentionally introduced nonlinearity can sometimes result in greater control capability or system functionality (1-2). Before smart material nonlinearities can be properly accounted for and/or utilized in control algorithms, system models and design strategies, their effect on system behavior must be better understood. This article reviews a preliminary study on the nonlinear behavior of a common smart material component, a 1-3 piezoceramic composite. The composite, shown in Figure 1a, consists of PZT-5 rods oriented in the thickness or 3 direction and uniformly separated by a compliant polymer material. Any change in the rod length due to the application of a voltage across the electrodes appears as a change in the thickness of the entire layer. Conversely, lateral strain is absorbed by the compliant material. The 1-3 is used in many applications, including medical diagnostic imaging, vibration isolation, structural acoustic control, nondestructive testing, and underwater acoustic sensing (3-5).

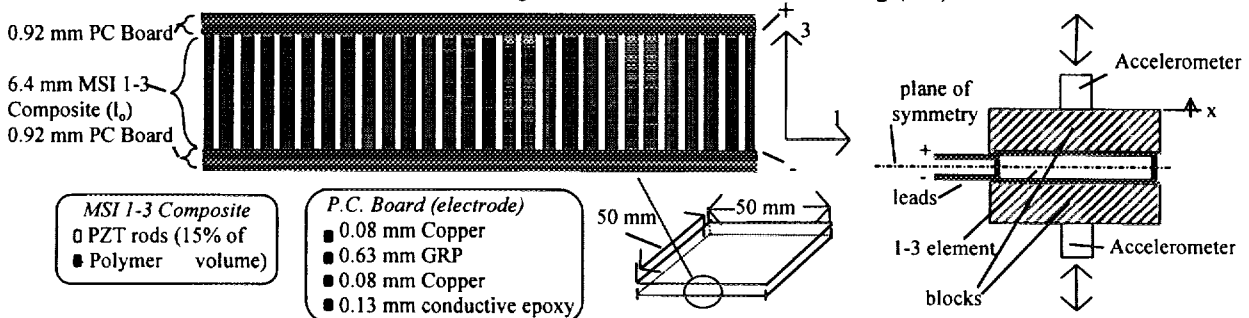

FIGURE 1. a) Cross section of 1-3 piezoelectric ceramic composite. b) Experimental test configuration.

Nonlinear constitutive equations for the 1-3 can be developed by merging prior nonlinear formulations for PZT (6) and prior linear formulations for 1-3's (7). For direct voltage drive of the test configuration shown in Figure 1b, an equivalent SDOF model is applicable.

$$m\ddot{x} + r\dot{x} + \left(c_1 + c_2 x + c_3 x^2 + \ldots - \gamma_1 V - \gamma_2 V^2 - \gamma_3 V x - \ldots\right)x + f_h[x, V, \dot{x}] = \left(e_1 + e_2 V + e_3 V^2 + \ldots\right)V \qquad (1)$$

Here, V is the applied voltage, x is the displacement, and m is the equivalent system mass. General expressions for mechanical linear viscous damping, r, and nonlinear hysteresis, f_h, have been added.

EXPERIMENT

Measurements of the dynamic response of the experimental test configuration to steady-state electrical sinusoidal excitation over a range of frequencies and amplitude levels were conducted. Sample results are shown in Figure 2. For Figure 2a, the resonant frequency of the configuration is beyond the displayed range. The first three harmonics

(fundamental and first two integer multiple higher harmonics) of the mechanical acceleration $\ddot{x}$ are shown for three different excitation voltage amplitude levels V, 70, 450 and 900 v (peak). Harmonic distortion of V was less than 0.01% at both levels. However, the amplitude-dependent harmonic distortion of $\ddot{x}$ reached 15%. Note the dominance of the third (symmetric) harmonic over that of the second. A linearized version of eq. (1) accurately predicts the fundamental harmonic response, but does not predict the higher harmonic content. Distortion levels are summarized in Table 1 with percentage values representing the contribution of all the dominant higher harmonics.

TABLE 1. Summary of Harmonic Distortion Levels for Figure 2a

Excitation Amplitude (v)	Distortion in terms of acceleration. Mean (range) %	Distortion in terms of velocity. Mean (range) %	Distortion in terms of displacement. Mean (range) %
900	15.6 (14.8 - 16.6)	5.7 (5.4 - 6.1)	2.2 (2.1 - 2.3)
450	7.7 (5.7 - 10.4)	2.8 (1.9 - 4.0)	1.1 (0.7 - 1.6)
70	2.2 (0.2 - 8.8)	0.7 (0.8 - 3.0)	0.2 (0.03 - 1.0)

In Figure 2b, a mechanical bias load of 1.1 kN and larger block masses were used, lowering the fundamental system resonance. Harmonic distortion in V remained below 0.1 %. Away from the system resonance, acceleration results look similar to Figure 2a. Near the resonance, there are differences with the asymmetric second harmonic more dominant than the third harmonic due to the bias load. Additionally, the resonant peak decreases in frequency at larger amplitudes, characteristic of a stiffness-softening nonlinearity or a stiffness-hardening nonlinearity under a bias load (8). Table 2 summarizes distortion levels and variability. The bias load and resonant dynamics have increased the overall level and variability of the harmonic distortion, behavior typical of nonlinear devices (9).

TABLE 2. Summary of Harmonic Distortion Levels for Figure 2b

Excitation Amplitude (v)	Distortion in terms of acceleration. Mean (range) %	Distortion in terms of velocity. Mean (range) %	Distortion in terms of displacement. Mean (range) %
900	28.3 (2.2 - 204)	11.6 (0.8 - 92.3)	5.0 (0.3 - 42.9)
450	14.1 (0.7 - 111)	5.8 (0.2 - 50.6)	2.5 (0.1 - 23.7)
90	2.5 (0 - 26.7)	1.1 (0 - 12.5)	0.5 (0 - 6.0)

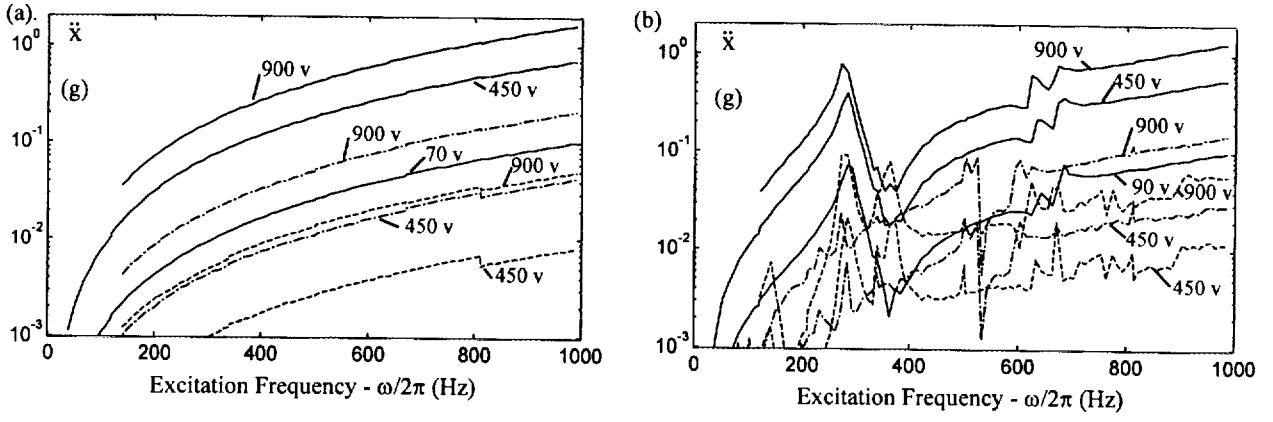

FIGURE 2. Mechanical response of experimental test configuration. Key: ———— first (fundamental), - - - - - - second, —·—·— third harmonic. a) Small equivalent mass. b) Large equivalent mass and bias load.

REFERENCES

1. Agnes, G. S., and Inman, D. J., *Smart Materials and Structures* **5**, 704-14 (1996).
2. Royston, T. J., and Singh, R., *Journal of Sound and Vibration* **194**, 295-316 (1996).
3. Corsaro, R. D., Houston, B. H., and Bucaro, J. A., *Journal of the Acoustical Society of America* **102**, 1573-81 (1997).
4. Smith, W. A., "The role of piezocomposites in ultrasonic transducers," *IEEE Ultrasonics Symposium*, 755-66, (1989).
5. Ting, R.Y., and Howarth, T. R., *SPIE Proceedings* **2721**, 214-21 (1996).
6. Joshi, S. P., *Smart Materials and Structures* **1**, 80-3, (1992).
7. Smith, W. A., *IEEE Transactions on Ultrasonics, Ferroelectrics and Frequency Control* **38**, 40-7, (1991).
8. Royston, T. J., and Singh, R., *Journal of Sound and Vibration* **198**, 279-98 (1996).
9. Royston, T. J., and Singh, R., *Journal of the Acoustical Society of America* **101**, 2059-69, (1997).